26.0 DEFORMATION MECHANISMS IN REFRACTORY-BASED, COMPLEX CONCENTRATED ALLOYS

Francisco Gil Coury (CSM)
Faculty: M.J. Kaufman, A.J. Clarke (CSM)
Industrial Mentors: Kevin Chaput, Todd Butler (AFRL)

26.1 Project Overview and Industrial Relevance

High Entropy Alloys (HEAs), Multi-Principal Element Alloys (MPEA), or Complex Concentrated Alloys (CCAs), are mixtures of 3 to 6 elements in near equimolar concentrations [26.1, 26.2]. The vast number of possible compositions results in a huge property landscape to explore. These alloys are of interest, due to their high strengths resulting from solid solution strengthening. Hundreds of alloys have already been studied to date. The most widely studied are 3-d transition metal CCAs. Other CCAs of interest include: refractory CCAs (RCCAs), lightweight CCAs, lanthanide CCAs, precious metal CCAs, brass and bronze CCAs, and C, N and B containing CCAs [26.1, 26.3–26.6]. Refractory CCAs, or RCCAs, are the focus of this work.

RCCAs are composed of mixtures of refractory elements, typically groups 4-6, along with Al, Cr and or Ti additions for oxidation/corrosion resistance. The microstructures of these alloys are usually composed of a simple body-centered-cubic (BCC) structure, sometimes present with other phases such as the ordered B2 phase [26.7], Laves phases [5,6] and hexagonal close packed (HCP) phases[26.8]. Most of these alloys display elevated solidus and liquidus temperatures. They also exhibit promising specific strengths, as well as high temperature and environmental performance [26.1], typically showing a better combination of properties than conventional refractory alloys. For structural applications, four properties are desirable, namely, strength, formability, corrosion/oxidation resistance and low density (especially for aeronautical and aerospace applications). It is well known that conventional refractory alloys are deficient in one or more of these properties. For example, Nb is one of the lighter refractory metals typically used in structural rocket engine components like nozzles and thrusters. Nb has good workability but is usually not as strong or oxidation resistant as other refractory metals. Therefore, expanding the number of RCCAs represents an opportunity for developing alloys with better property combinations.

Although promising, the data available so far for RCCAs is limited. For example, most of the mechanical tests conducted to date have been simple compression tests, which might overestimate the ductility and toughness of these alloys. Thus, there is essentially no knowledge about the fatigue, creep, or fracture toughness properties that are clearly relevant for structural applications at high temperatures. Furthermore, few models or studies are available concerning RCCA deformation mechanisms, and whether they differ from conventional BCC alloys. On a final note, although it is generally accepted that solid solution strengthening is predominant in RCCAs, few models are available in the literature that predict the magnitude of this hardening. This study is focused on understanding the strength and deformation behavior of RCCAs. Clarification of these properties would not only aid in the understanding of other properties such as ductility, toughness, fatigue and creep, but should also enable more effective alloy design.

26.2 Previous Work

The first step in this project was alloy selection. A total of 11 criteria were imposed on quaternary equiatomic mixtures of refractory elements plus Cr, Ti and Al and a total of 13 alloys were selected with the aid of thermodynamic calculations using Thermo-Calc®. One of the criteria was that the alloys should have a single-phase BCC microstructure at some temperature range before melting. The criteria also considered factors such as cost and processability of these alloys. The selected alloys were then produced by the member company ATI. In the meantime, some additional NbTaTiX compositions were produced by arc-melting. These latter alloys were characterized by scanning electron microscopy (SEM) and transmission electron microscopy (TEM) to identify the phases present in the as-cast condition and all were single phase BCC. Also, as pointed out in the previous report, the Toda-Caraballo (TC) [26.9, 26.10] model was used to predict the strengths of all the alloys produced. The TC model allows a quick assessment of the strength of CCAs by inputting the elastic properties and atomic radii of the elements and the composition of the alloy. A primary goal of this project is to access the validity of the TC model and determine whether adjustments are needed in order to provide better strength predictions by comparing predictions to measured properties from the selected alloys. This comparison should not only show whether the TC model is a valid tool for predicting the strength of RCCAs but also clarify the fundamentals of the solid solution strengthening mechanisms operating in these multicomponent alloys.

26.3 Recent Progress

26.3.1 Characterization of the As-Cast and Heat-Treated Samples

After casting, ATI sent a piece of each of the 11 alloys for microstructural analysis by x-ray diffraction (XRD), SEM and TEM. For the sake of simplicity, all the alloys were divided into 3 families, namely, those containing NbTaTi, those containing Al, and those containing Cr. The alloys were characterized in the as-cast condition and after a heat-treating step consisting of 5 cycles of 7 h at 1400 °C under vacuum followed by furnace cooling to room temperature. The results are summarized in **Fig. 26.1**, in which the XRD patterns of all the alloys are shown.

Empirical thermodynamic phase prediction criteria (the δ and Ω parameters) were applied to the alloys produced in this work. The predicted values can be better visualized if plotted on a δ versus Ω plot. In the literature, there are usually threshold values used to predict whether an alloy will exist as a disordered solid solution at all temperatures. δ versus Ω plots for the heat-treated experimental alloys and several alloys from the literature are shown in **Fig. 26.2**. Usually the δ versus Ω plot is constructed for all types of HEAs plotted together. As shown here, if we only plot RCCAs, we can see that the single-phase region predicted by the empirical parameters for these alloys (within orange box) seems to be smaller than the region for the entire HEA alloy class (within orange box). This is most likely a consequence of the particularities of the RCCAs with respect to the other HEAs, namely, their high melting points and their tendency to form BCC phases. Many of the non-refractory HEAs studied to date are made from transition elements with substantially lower melting points and FCC structures. RCCAs are typically BCC and competing phases are HCP, ordered versions of BCC (such as B2) and other phases (Laves and A15), as shown **Fig. 26.1**. Therefore, considering the empirical nature of these predictions, it is not surprising that these alloys have their own set of threshold values.

Since we are mostly interested here in studying the solid solution strengthening fundamentals of these RCCAs, the main focus of this work is on the mechanical properties of single-phase compositions in order to isolate this effect from other strengthening effects. Therefore, focus will be given in this report to the single-phase compositions.

Starting with the NbTaTi family, some alloys that were single phase in the as-cast state had multiple phases after the heat treatments. For example, the AlNbTaTi and CrNbTaTi alloys contained significant amounts of secondary phases, namely, a Cr-rich Laves phase in CrNbTaTi and an Al-rich A15 phase in AlNbTaTi. The other three alloys from this family (MoNbTaTi, WNbTaTi and HfNbTaTi) did remain single phase (BCC) after the heat treatment. Among this latter group, only the HfNbTaTi alloy is ductile at room temperature. This alloy was selected for hot rolling by ATI and the hot-rolled sample will be used for extracting tensile coupons. The single-phase alloys that were relatively brittle at room temperature (MoNbTaTi and WNbTaTi alloys) will be studied in compression for comparison.

For the Cr-containing family, none of the alloys were single phase after the heat treatment except for the CrNbMoTi alloy. Additionally, the CrMoTaTi displayed a small amount of a C15 Laves phase, around 6 wt%, quantified by Rietveld refinement in synchrotron XRD patterns. In any case, these alloys will also be incorporated in this study by using compression tests.

Lastly, the Al-containing HfAlNbTi and HfAlTaTi alloys were single-phase B2 after heat treating whereas the AlMoNbTi alloy, which was single phase on the as-cast condition, contained some of the A15 phase upon heat treatment similar to the AlNbTaTi alloy mentioned previously.

As a first estimate of how the strengths of the RCCAs increase with the atomic size mismatch and elastic modulus mismatch of the alloy, the hardnesses of these alloys were compared to calculated values for these two parameters (**Fig. 26.3**). As can be seen, there is no obvious correlation between these two parameters and hardness, not even when a combination of both is attempted. This indicates that the approach of extracting the thermal and athermal components of the deformation behavior might be more promising than interpreting the strength at room temperature based only on the classical atomic size and elastic modulus mismatches.

26.3.2 Testing the BCC materials at different temperatures

Some of the single-phase alloys produced in this work were tested in a Gleeble® mechanical simulator. Cylindrical samples of 3mm in diameter by 6mm in height were machined by electro-discharge machining (EDM) from the heat-treated alloys. The mechanical tests were performed under a strain rate of $10^{-3}s^{-1}$. Different temperatures were chosen in the interval between room temperature and 1000 °C. To date, only the MoNbTaTi alloy has been tested and the full set of stress-strain curves are included in **Fig. 26.4**. For this alloy, the results indicated that, as expected, the yield

stress decreases with increasing temperature. This drop is plotted in **Fig. 26.5** where it is apparentl that the yield stress drops rapidly as the temperature in increased from room temperature. At around 600 °C, the alloy reaches the athermal plateau, as can be seen by the small difference in the yield strength between the 600 and 800 °C tests. For the 1000 °C test, the thermocouple was dislodged during the test thereby explaining the odd curve at this temperature.

In summary, the tests performed here show that the athermal slip barrier for this HEA is much larger than that in conventional refractory alloys. For example, pure Nb, which has relatively similar melting temperature (2477 °C) compared to the MoNbTaTi alloy (2440 °C liquidus temperature), reaches the athermal plateau at a much lower temperature (RT) than the HEA studied here (~600 °C).

26.4 Plans for Next Reporting Period

Mechanical testing will be finalized and a model for thermally-activated deformation will be developed for the RCCAs. The thermally-activated deformation of these alloys will be compared to the parameters, such as the activation energy and lattice resistance at 0K, expected for conventional alloys from the literature. The strengths of the different RCCAs will be correlated with composition using strength models from the literature in an effort to capture how well these models predict the strengths of these alloys and, for the cases where the predictions are inaccurate, evaluate how they can be improved.

26.5 References

[26.1] D.B. Miracle, O.N. Senkov, Acta Mater. 122 (2017) 448–511.

[26.2] Y.F. Ye, Q. Wang, J. Lu, C.T. Liu, Y. Yang, Mater. Today 19 (2016) 349–362.

[26.3] O.N. Senkov, S. V. Senkova, C. Woodward, Acta Mater. 68 (2014) 214–228.

[26.4] O.N. Senkov, J.M. Scott, S. V. Senkova, F. Meisenkothen, D.B. Miracle, C.F. Woodward, J. Mater. Sci. 47 (2012) 4062–4074.

[26.5] O.N. Senkov, C.F. Woodward, Mater. Sci. Eng. A 529 (2011) 311–320.

[26.6] O.N. Senkov, S.V. Senkova, D.B. Miracle, C. Woodward, Mater. Sci. Eng. A 565 (2013) 51–62.

[26.7] Y. Ma, B. Jiang, C. Li, Q. Wang, C. Dong, P. Liaw, F. Xu, L. Sun, Metals (Basel). 7 (2017) 57.

[26.8] S. Maiti, W. Steurer, Acta Mater. 106 (2016) 87–97.

[26.9] I. Toda-Caraballo, Scr. Mater. 127 (2017) 113–117.

[26.10] I. Toda-Caraballo, P.E.J. Rivera-Díaz-Del-Castillo, Acta Mater. 85 (2015) 14–23.

26.6 Figures and Tables

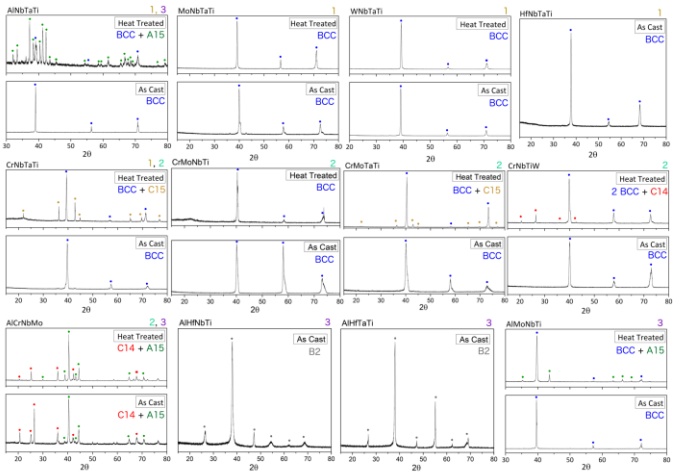

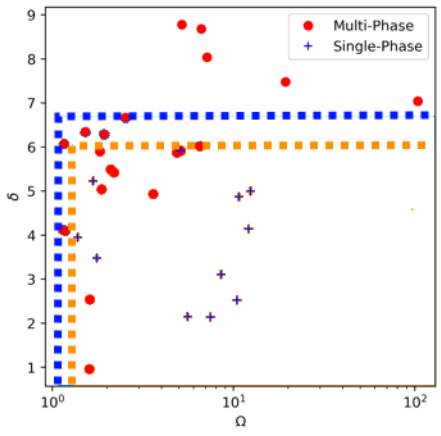

Figure 26.2: Plot of the δ and Ω thermodynamic parameters for several

Figure 26.1: Indexed XRD patterns of all alloys produced in this work in the as-cast and heat-treated conditions.

different RHEAs in the heat-treated condition.

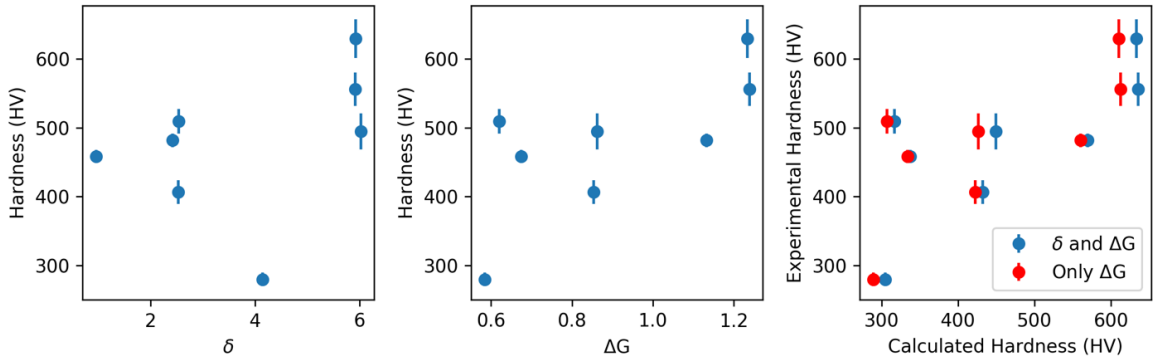

Figure 26.3: Plots of the different parameters versus the hardness of the single-phase alloys: The atomic size mismatch delta (a), the elastic modulus mismatch (b) and a combination of both for predicting the hardness (c).

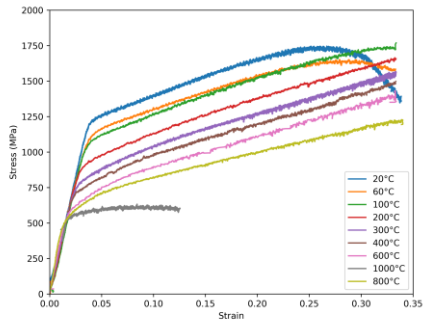

Figure 26.4: Stress-strain curves of MoNbTaTi alloys produced in this work at different temperatures

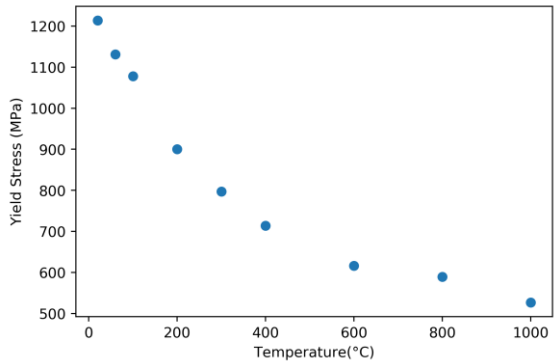

Figure 26.5: Yield strength-temperature plots of the alloys produced in this work